

## **ANALYSIS OF SUPERPLASTIC FORMING PROCESS APPLIED TO AEROSPACE INDUSTRY: CASE STUDY OF Al 5083 ALLOY**

D. A. Pereira<sup>1</sup>, M. H. F. Batalha<sup>1</sup>, A. F. Carunchio<sup>1</sup>, H. B. Resende<sup>1</sup>

<sup>1</sup> *Institute for Technological Research, Lightweight Structures Laboratory, São José dos Campos 12247-016, SP, Brazil*

### **ABSTRACT**

Superplastic forming (SPF) is a method especially useful for obtaining complex and precise lightweight metal components, which is achieved at a particular range of strain rates and temperature. One of its advantages is the capacity to produce complex parts in a single operation with a great surface finish, what implies in weight savings as opposed to traditional processes. Moreover, there are slight or no residual stress and “spring back” effects, leading to a high-quality structural integrity. The SPF has been widely used in aerospace applications due to the demand for structures with an optimum specific strength, stiffness and lightweight. In the aerospace industry, the most common applications of SPF use aluminum alloys (2XXX, 5XXX, 6XXX, and 7XXX) for lightly loaded or non-structural components, such as inlets, wing tips, access doors and equipment covers. The development of aeronautical market increases the need for high volume production, and as a consequence, it is raising the competition between proper forming technologies. In this context, the study of the SPF methodology can reach the following goals: (i) reduction of process time and (ii) enhancing the quality of the product. It is known that the control of variables like the gas pressure, the temperature and the grain size are relevant to increase the strain rate and improve the output properties, therefore, research and development in this area are desirable. This work presents a study of the SPF process analyzing the quality of the final product using a particular pressure curve to form an AA5083 alloy bubble shape. The study shows a numerical model to calculate the optimized cycle of an Accudyne© SPF machine. The paper also discusses the quality of product analyzing the smooth and symmetry characteristics of the material through ultrasound technique. The results showed a uniformity of the material around the bubble. The relatively small cycle time of the optimized pressure curve leads to an attractive forming method for the aerospace market niche. Highlighting SPF is a process that must be considered to produce a new generation of lightweight size products presenting complicated design.

**Keywords:** *superplastic forming, aluminum 5083, aerospace*

## INTRODUCTION

The superplastic process (SPF) is a forming technique useful to manufacture structural components with a complex shape, especially in metals alloys such as titanium, magnesium and aluminum. It exhibits numerous technical and economic advantages for manufacturing laborious part geometries, which enables the potential of lightweight production (Kappes and Liewald 2011). An easy way to apply SPF is by the blow forming process, which consists of a single sheet laid on a female die subjected to gas pressure resulting in a formed part with the die configuration (Giuliano 2011). The technique has this name due to the capability of some metal alloys, under specific conditions, to reach high elongation; some of them more than as 2000%, without forming a neck, which is associated with failure. However, in this condition, the flow stress is very sensitive to the strain rate; therefore, the superplasticity envelope should be studied carefully. There are three primary conditions necessary for determining this envelope: the temperature, the strain rate, and the grain size of the alloy. The process temperature is in order of  $\sim 0.5T_m$ , where  $T_m$  is the absolute melting temperature of the material. Besides that, this process happens just in a few range of strain rate, usually between  $10^{-4}$  and  $10^{-3} \text{ s}^{-1}$ . Finally, the microstructure should have a fine and stable grain size. Thus, the grain sizes used for materials in the superplastic forming industry are generally in the range of  $\sim 2\text{--}10 \text{ }\mu\text{m}$ . This requirement exists due to the physical behavior of the process, obtained owing to the occurrence of intensive grain boundary sliding (GBS), which is believed to be the principal deformation mechanism (Alabort et al. 2016). The GBS is well explained in Kaibyshev (2002), and it is associated with a series of accommodation mechanisms as, for example, the grain boundary migration, grain rotation, recrystallization, diffusional mass transport and slip in grains (Sieniawski and Motyka 2007), which may depend on upon important alloy characteristics such as phase architecture and grain morphology. In a simple explanation, the basic difference between plastic deformation and superplastic deformation is showed in Figure 1.

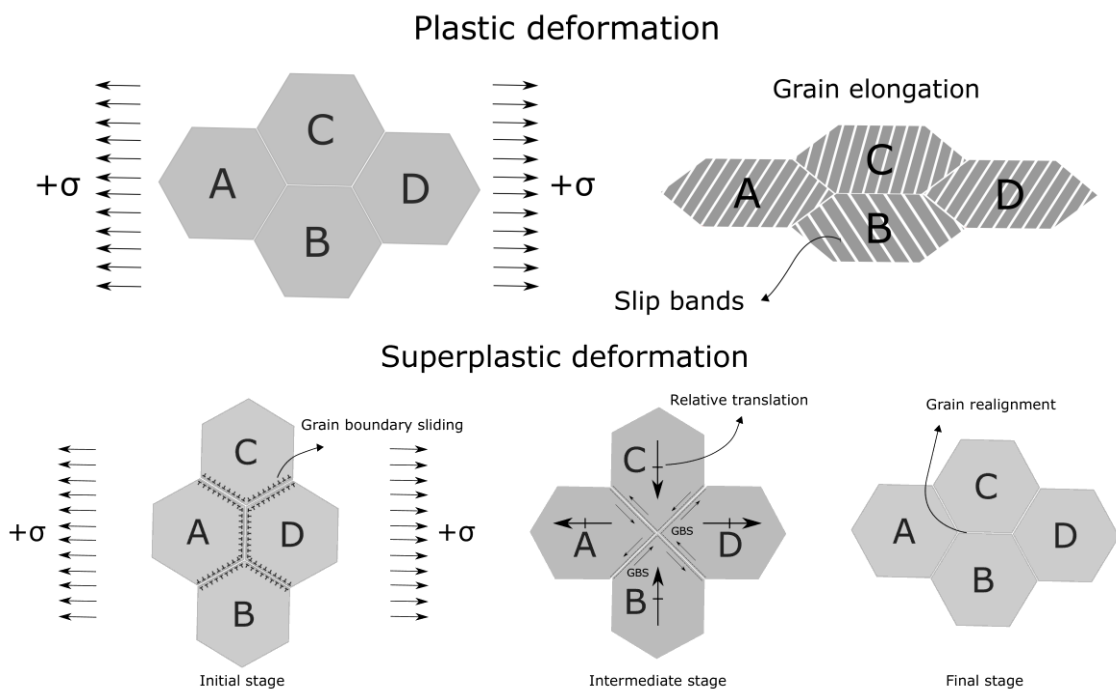


**Figure 1. Comparison between plastic and superplastic deformation regarding intragranular modification.**

Superplastically formed components are used because they meet functional and market needs and are competitively priced (Barnes 2007). Barnes (2007) wrote an excellent review of the history and applications of the SPF forming during the last few decades. The main advantages of the SPF process are the capacity to produce complex and multiple parts in one operation with a great surface finish, i.e. it may dispense welding and machining, and it can manufacture a series of products using only one tooling. Due to the capability of achieving high strains, SPF enables the production of otherwise difficult-to-manufacture or not-manufacturable part geometries. Moreover, there are slight or no residual stress and “spring back” effects, leading to a high-quality structural integrity. For that reason, SPF can result in considerable savings in costs and weight as opposed to traditional processes which make the method feasible and attractive for industry. Low flow stresses, generally <10 MPa combined with the relatively high uniformity of plastic flow, have led to increasing commercial interest in superplastic forming (Giuliano 2011). This characteristic associated with low forming speeds make SPF very attractive especially for small lot sizes; the aeronautical industry is an example of the attractive market.

One of the main challenges of superplastic forming is to increase the productivity of manufacturing, but also to expand its range of applicability (Barnes 2007), which means decreasing the forming temperature and reducing the forming time. In titanium alloys, for example, this is achieved optimizing the microstructure by refining the grain size (Salishchev et al. 2012) and by increasing the  $\beta$  fraction (Meier, Lesuer, and Mukherjee 1992). The idea is to improve the microstructure characteristics for SPF and the composition of the alloy to accelerate the process conditions outside the optimal envelope of superplastic formability, which is considered the region with the highest strain rate coefficient ( $m$ ), i.e., the concept is to form the material at lower  $m$  index. Figure 2(a) shows the log-log graph of the stress-strain rate relation for a standard and superplastic materials; one can recognize that there are three regions I, II and III, which depends on the strain rate velocity. Fig. 2(a) also presents the equation to calculate  $m$  which is the angular coefficient of the curve, while figure 2(b) shows the strain rate coefficient vs. the log of the strain rate.

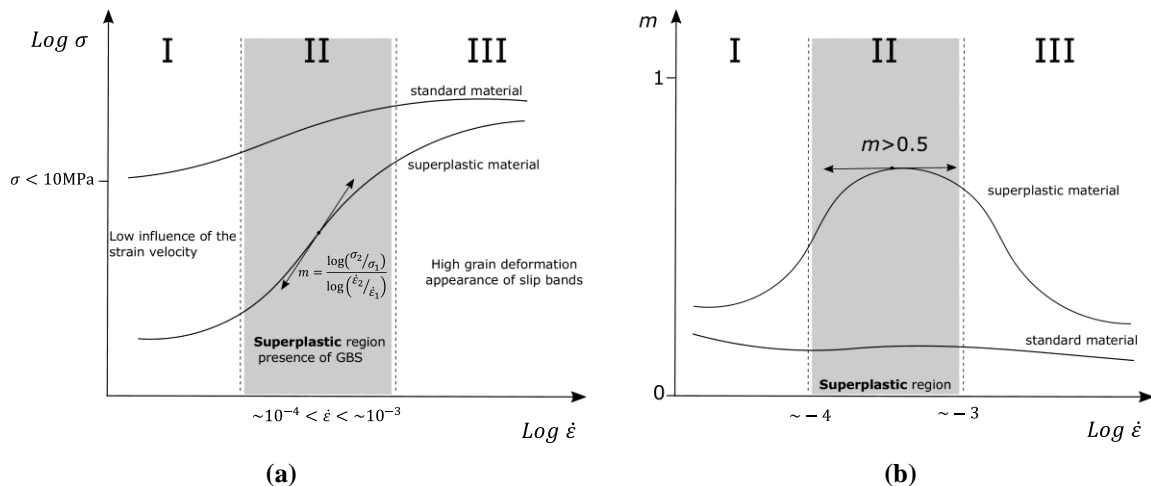


**Figure 2. (a) The relation between the stress and strain rate divided into three different regions and the method to calculate the strain rate sensitivity; (b) strain rate vs. strain rate coefficient.**

In Figure 2, one can see that the superplastic materials have the higher  $m$  values in segment II, called here as a superplastic region, which presents the GBS behavior. In the region III, the strain rate is too fast for the SPF envelope, and the grain gives a high deformation with a strong presence of slip bands (*cf.* Fig. 1). The region I shows weak influence of the strain velocity, and it is common to have the grain growing due to the low speed which reduces the  $m$  value. Figure 2(b) shows the strain rate coefficient vs. the log of

the strain rate; one can conclude that the highest values of  $m$  are present in the region II for the superplastic materials, which show rates greater than 0.5.

The most conventional superplastic materials with commercial applications are the titanium and aluminum alloys. The most common applications for Ti alloys in the aeronautical industry are pylon panels, nacelle panels, engine parts, fan and OGV blades; and for the Al alloys are lightly loaded or non-structural components, such as inlets, wing tips, access doors and equipment covers. Barnes (2007) gives a review of some commercially available superplastic sheets. Kawasaki and Langdon (2007) lists and examines various reports of superplasticity in ultrafine-grained materials. Table 1 shows the most common alloys, its composition, SPF temperature, strain rate and maximum deformation.

**Table 1.** Commercially available Ti and Al superplastic sheet with optimum SPF temperatures, strain rates and typical elongations, adapted from Giuliano (2011).

	Alloy	Composition, wt%	SPF temperature	Strain rate	Elongation
Titanium	Ti-6/4	Ti-6Al-4V	880-920°C	$5 \times 10^{-4} s^{-1}$	~1000%
	SP700	Ti-4Al-3V-2Fe-2Mo	750-800°C	$3 \times 10^{-4} s^{-1}$	≥ 300%
	Ti-6242	Ti-6Al-2Sn-4Zr-2Mo	850-940°C	$5 \times 10^{-4} s^{-1}$	> 500%
	IMI550	Ti-4Al-4Mo-2Sn-0.5Si	880-900°C	$5 \times 10^{-4} s^{-1}$	> 500%
	IMI834	Ti-5.8Al-4Sn-3.5Zr-0.7Nb-0.5Mo-0.3Si-0.05C	950-990°C	$\sim 10^{-4} s^{-1}$	~300%
Aluminum	2004	Al-6Cu-0.4Zr	460°C	$\sim 10^{-3} s^{-1}$	800 – 1200%
	5083	Al-4.5Mg-0.7Mn-0.1Zr	500-520°C	$10^{-3} s^{-1}$	~300%
	7475	Al-5.7Zn-2.3Mg-1.5Cu-0.2Cr	515°C	$2 \times 10^{-4} s^{-1}$	800%
	8090	Al-2.4Li-1.2Cu-0.7Mg-0.1Zr	530°C	$5 \times 10^{-4} s^{-1}$	1000%
	2090	Al-2.5Cu-2.3Li-0.12Zr	530°C	$\sim 10^{-3} s^{-1}$	~500%

More than 40 “in-production” aircraft and twenty different automobiles are using superplastically formed aluminum components (Barnes 2007). According to Barnes et al. (2012), among all of the commercially available superplastic alloys, AA5083 is the most widely used, amounting to many thousands of tons per year. The efforts to increase the superplastic alloy properties created a new material called SP5083, which follows aerospace standards. This non-heat treatable medium strength alloy combined with suitable configuration has allowed an increasing number of aerospace SPF components. The important attributes of both SPF design; the ability to create complex geometry, and the excellent post-formed characteristics of SP5083 that have created cost-effective solutions to specific Aerospace Industry needs (Barnes et al. 2012). Hefti (2007) discuss the Boeing implementation of the SP 5083 and the advances that have been made at Boeing Commercial Airplanes during the manufacture of SPF aluminum components for aircraft applications. He highlights that this material is the lowest cost aluminum alloy that exhibits superplastic properties once the cost of heat treating, quenching, and aging is avoided. According to him, SP5083 components can reach the structural requirements for a particular number of elements even though a low strength alloy. Consequently, it has replaced aluminum castings, fiberglass assemblies, and components fabricated by SPF from other aluminum alloys, which make this alloy widely implemented on various Boeing commercial airplanes. Figure 3 gives an example of SP5083 aeronautical components used in Boeing 737 and Boeing 777.

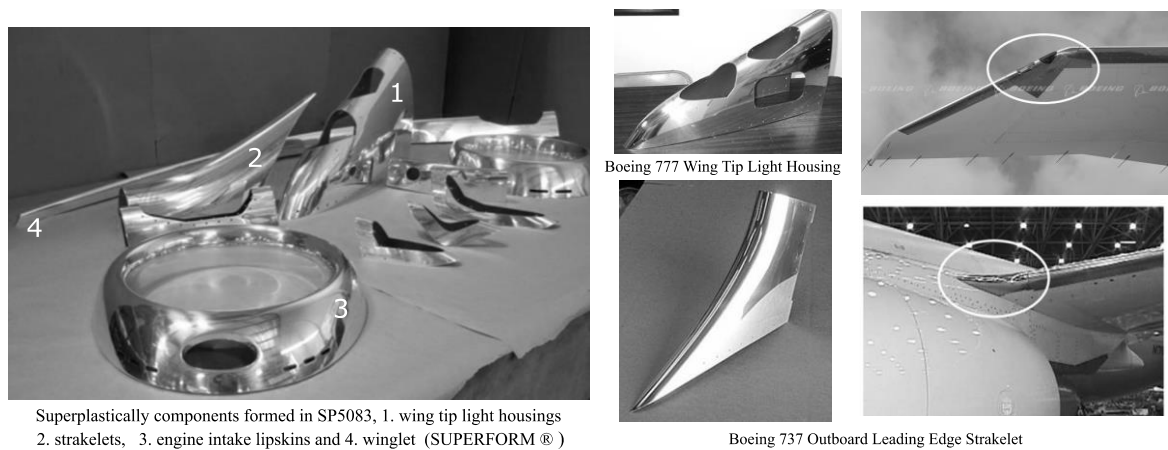


**Figure 3. Superplastic components using SP5083 designed for aerospace applications, adapted from Barnes et al. (2012) and Hefti (2007).**

Many authors have been studying the AA5083 and its properties related to the superplastic forming technology. Kappes and Liewald (2011) deal with a pneumatic bulge test, setting a constant pressure profile using aluminum alloy 5083. They measured the strain of the bulging in situ to obtain the real parameters, as the strain-rate sensitivity index ( $m$ ), using the least square error method. The comparisons between the experimental and numerical results using the actual parameters have shown good correlation. The conclusions are relevant to determine superplastic materials and process parameters accurately and efficiently, permitting designing SPF processes in an industrial environment. Aksenov et al. (2015) proposed a method for determination the real material characteristics using the inverse analysis of a bulging tests result. They performed a lot of analysis using a constant pressure profile, in each experiment they have identified the relation between the height of the dome and its thickness. The proposal technique has shown a useful tool to determine the material constants, which can be applied to optimize the SPF parameters for industrial applications.

Although the AA5083 has a reasonable combination of cost, forming, and processing characteristics, a significant problem with this alloy is the internal micro-void formation during superplastic deformation, which is usually called cavitation. This problem is responsible for decreasing the structural integrity of the part and in some cases it can guide to a crack initiation that invalidates the component. Therefore, to avoid high levels of cavitation, in actual parts designed for AA5083, equivalent strain levels (EqSL),  $EqSL = \left[ \left( \frac{t_0}{t_{min}} - 1 \right) 100 \right]$  are usually limited to 150%. In structural components where the containment of cavitation is important, EqSL should be restricted to 100% to ensure cavity volume fraction does not exceed 0.5% (Sun et al. 2009). If higher EqSLs are required, back pressure forming may be necessary (Gershon et al. 2004). Sun et al. (2009) studied the effect of lubrication on the cavitation level evolution, thickness distribution, and void distribution in the bulging SPF process of an aluminum alloy 5083, comparing with and without lubrication. They have shown that the maximum void volume fraction could be actually reduced by forming with lubrication.

It is reasonable to think that SPF is one of the greatest technologies to form lightweight parts. During the last decades, many authors have been studying the importance and application of the SPF process in different alloys, the industry has shown a high interest in aluminum alloys, and the AA5083 has been widely used. Therefore, due to the needs of the industry and the great capacity of the SPF process, more studies should be carried out to understand the phenomenon with the objective of reducing the forming time, improve the

structural characteristics and, finally, avoid cavitation in the AA5083. Hence, the purpose of this work is to study the influence of the pressure curve, temperature, strain rate and the cavitation phenomena in the AA5083 alloy bubble shape. The study presents a numerical model to calculate the optimized cycle of an Accudyne© SPF machine. The paper also presents the quality of product analyzing the smooth and symmetry characteristics of the material through ultrasound technique. The SPF mechanism is established in the Lightweight Structures Laboratory (LEL), which is a laboratory of the Institute for Technological Research (IPT) located in Sao Jose dos Campos, Brazil. The focus of the lab is to support industry in R&D, helping it to pass through the Death Valley in the Technology Readiness Level, assisting them to become more competitive, getting results close to real application.

## METHODS

During the SPF process, it is important to make sure about the strain rate and temperature values, because those two parameters, as mentioned previously, have a strong influence in the deformation mechanism. Therefore, to guarantee the grain boundary sliding for AA5083 alloy, it is important to have the temperature between 500°C and 525°C, and the strain rate between  $10^{-4} \text{ s}^{-1}$  to  $10^{-3} \text{ s}^{-1}$ . To obtain this condition, an analytical model with corrections for the hardening effect is applied, in order to obtain the best configuration for the pressure curve and, finally, be possible to reach the superplastic window.

The free body diagram of the forming process is presented in Figure 4, where P is the applied pressure, r is the radius of the curvature and  $\sigma_1$  is the hoop stress.

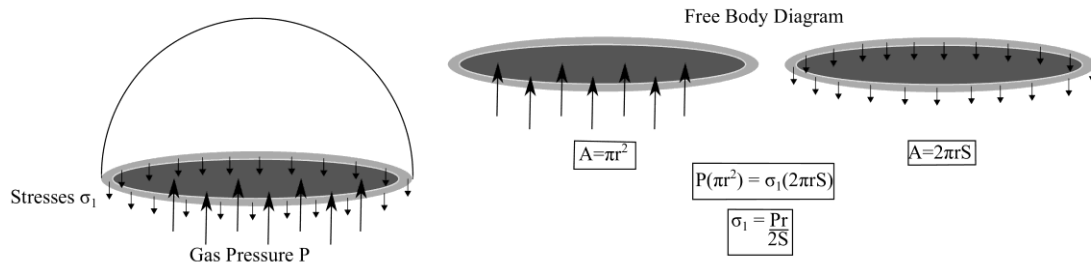


**Figure 4 – Free body diagram of the forming process necessary to drive the equations.**

Starting from the formulation given by Dutta and Mukherjee (1992) one can follow those equations:

$$P = 2 \frac{S}{r} \sigma_1 \quad [1]$$

Where  $S$  is the thickness of the sheet. Applying the Von Mises effective stress criterion, the effective stress is given by:

$$\bar{\sigma} = \frac{1}{(2)^{1/2}} [(\sigma_1 - \sigma_2)^2 + (\sigma_2 - \sigma_3)^2 + (\sigma_3 - \sigma_1)^2]^{1/2} \quad [2]$$

Where  $\sigma_2$  is the meridional stress and  $\sigma_3$  is the stress in the thickness direction, which in this case is zero because of the thin membrane. From symmetry,

$$\sigma_1 = \sigma_2 \quad [3]$$

Substituting the eq. 3 in 2, one obtain

$$\sigma_1 = \bar{\sigma} \quad [4]$$

The thickness of the membrane after  $t$  time can be written as:

$$S = S_0 e^{-\dot{\varepsilon}_3 t} \quad [5]$$

Where  $S_0$  is the instantaneous thickness of the membrane, and  $\dot{\varepsilon}_3$  is the thickness strain rate. To calculate  $\dot{\varepsilon}_3$ , one can consider the principal stresses and strains related by Nadai's equation (Jones 2009) as follows:

$$\varepsilon_1 = \frac{1}{E_p} \left[ \sigma_1 - \frac{\sigma_2 - \sigma_3}{2} \right] \quad [6]$$

$$\varepsilon_2 = \frac{1}{E_p} \left[ \sigma_2 - \frac{\sigma_1 - \sigma_3}{2} \right] \quad [7]$$

$$\varepsilon_3 = \frac{1}{E_p} \left[ \sigma_3 - \frac{\sigma_1 + \sigma_2}{2} \right] \quad [8]$$

Where  $E_p$  is the plastic modulus,  $\varepsilon_1, \varepsilon_2$  and  $\varepsilon_3$  are the hoop strain, meridional strain and the thickness strain respectively.

From the equation 6, 7 and 8, one can show that:

$$\varepsilon_1 = \varepsilon_2 \quad [9]$$

$$\varepsilon_3 = -2\varepsilon_1 \quad [10]$$

From Von Mises's effective strain criterion, the effective strain  $\bar{\varepsilon}$  can be written as:

$$\bar{\varepsilon} = \frac{(2)^{1/2}}{3} [(\varepsilon_1 - \varepsilon_2)^2 + (\varepsilon_2 - \varepsilon_3)^2 + (\varepsilon_3 - \varepsilon_1)^2]^{1/2} \quad [11]$$

Substituting the equations 9 and 10, the equation 11 becomes:

$$\varepsilon_3 = \bar{\varepsilon} \quad [12]$$

Therefore, deriving in time the equation 12, one can obtain:

$$\dot{\varepsilon}_3 = \dot{\bar{\varepsilon}} \quad [13]$$

From the constancy volume:

$$AS = A_0 S_0 \quad [14]$$

Where  $A$  and  $A_0$  are the initial and instantaneous areas of the sheet, respectively.

The area of a membrane with a radius of curvature  $r$  at any instant can be writing in terms of the die radius ( $a$ ) as:

$$A = 2\pi r \left[ r - (r^2 - a^2)^{1/2} \right] \quad [15]$$

Substituting the values of  $S$  and  $A$  in the equation 15 by the equations 14 and 5 one can obtain:

$$2\pi r \left[ r - (r^2 - a^2)^{1/2} \right] S_0 e^{-\dot{\varepsilon}_3 t} = \pi a^2 S_0 \quad [16]$$

Hence,

$$r = \frac{a}{2[e^{-\dot{\varepsilon}_3 t}(1 - e^{-\dot{\varepsilon}_3 t})]^{1/2}} \quad [17]$$

Combining the equations:

$$\frac{S}{r} = \frac{2S_0 e^{-\dot{\varepsilon}_3 t} [e^{-\dot{\varepsilon}_3 t}(1 - e^{-\dot{\varepsilon}_3 t})]^{1/2}}{a} \quad [18]$$

The final equation for the pressure is:

$$P = 4 \frac{S_0}{a} \bar{\sigma} e^{-\dot{\varepsilon}_3 t} [e^{-\dot{\varepsilon}_3 t}(1 - e^{-\dot{\varepsilon}_3 t})]^{1/2} \quad [19]$$

The effective stress ( $\bar{\sigma}$ ) and effective strain rate ( $\bar{\dot{\epsilon}}$ ) can be replaced by the uniaxial parameters (Dutta and Mukherjee 1992). However, it is essential to update the effective stress continuously in Dutta and Mukherjee's equation, in order to account for the strain hardening (Deshmukh 2003). The value of  $\bar{\sigma}$  is corrected by the uniaxial stress  $\sigma$  in each step of time follow the polynomial equation with is the fit of the real stress-strain curve in that range of temperature and strain rate.

The machine used in the experimental procedures, presented in Figure 5, works with a system range of 15 to 150 Ton of hydraulic clamp force, and has a work area of approximately  $760 \times 860$  mm. The gas pressure, which presses the blank against the die, has a range of 1 to 40 Bar, and can work with gas injection in both sides of the blank (a necessary condition for any work using back pressure). The control system allows different values of gas level step, ramp gas rate, dwell time and clamp force, during forging process, what should be specified according to final part geometry and material.



**Figure 5 –Lightweight Structures Laboratory's superplastic forming Accudyne machine.**

About of the forming process, it has followed the steps that are present below and depicted in Figure 6.

- I. Initially the press was heated until reach the desirable temperature, in this case  $500^{\circ}\text{C}$ ;
- II. The blank disk, that is compatible with SPF tool, was coated with boron nitride to avoid the part sticking in metal tooling, as a recommendation of the machine's manufacturer. Furthermore, previous trials of forming without boron nitride have led to difficulties to extract the formed from the die;
- III. The press was opened and the part put on it;
- IV. The homogeneous time, that is, the time necessary for the blank reach the desirable temperature, was waited.
- V. The up part of the press was sent down to clamp the blank's edge, in order to seal the blank against the die and prevent the gas to escape;
- VI. Finally the gas flow followed the pressure  $\times$  time curve, forming the part.

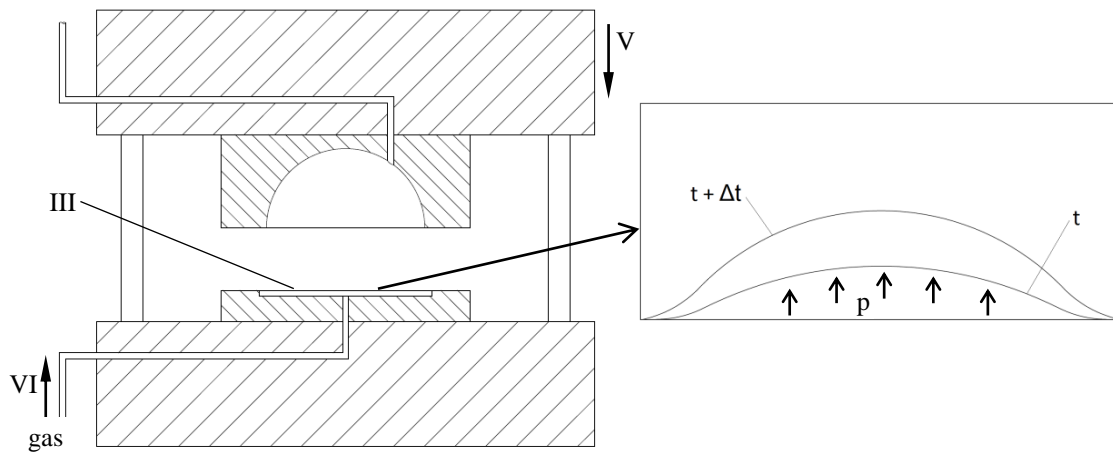


**Figure 6 – Superplastic press and forming scheme.**

The samples were inspected with ultrasonic scanning to verify if the process guarantee homogeneous thickness reduction. The equipment used was an Olympus Omniscan SX: type UT, mode pulse-echo, sound velocity of 6172.8 m/s, 27 dB Gain and transducer generates longitudinal waves at 5MHz. It was measure in 17 points over its cross-section, shown in Figure 7.

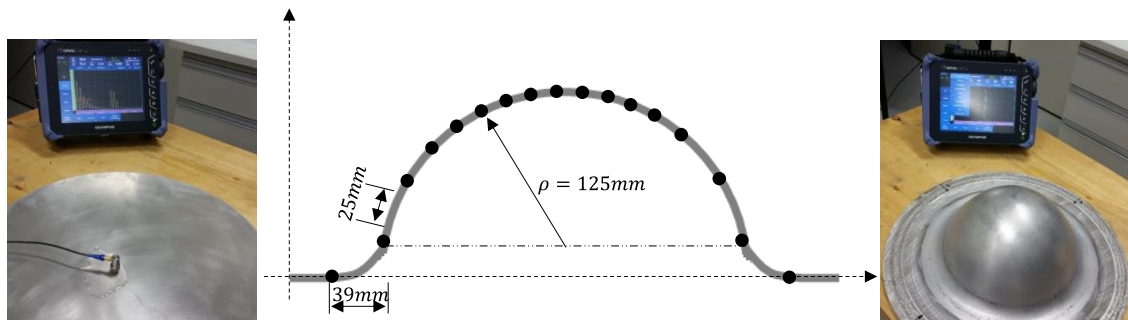
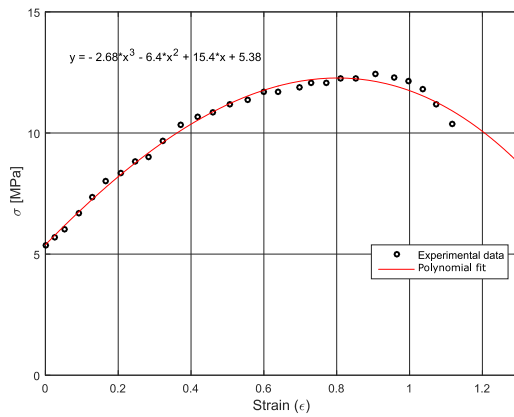


**Figure 7- Ultrasonic inspection equipment and measured points.**

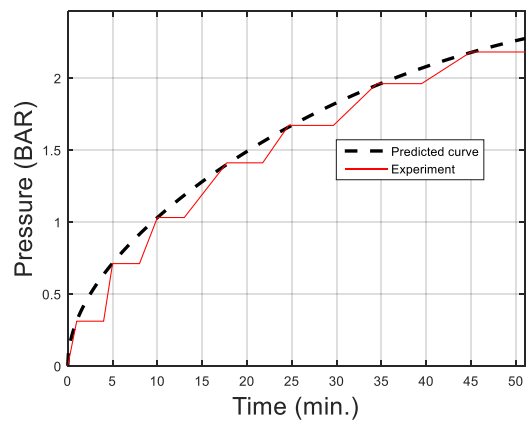
In order to give a better view of the material behavior, it was also done a preliminary microstructural-crystallographic characterization, which compares microstructure before and after forming process. The area inspected was next to the center of the dome, that represents a critical zone regarding high strain levels. Two techniques were used, orientation mapping by electron backscatter diffraction (EBSD) and sample's surface topography by scanning electron microscope (SEM).

## RESULTS AND DISCUSSION

Figure 8(a) gives the uniaxial stress-strain curve and the polynomial fit from the experimental results necessary to correct the hardening effect in the numerical model; the experimental curve was obtained from the Jarrar et al. (2012). The pressure curve obtained through Dutta and Mukherjee (1992) analytical model was adjusted to 14 linear functions, the only type of function that is accepted as a input by the hot press control system. The results are depicted in figure 8 (b). The experimental process, using the ajusted curve, was concluded after 51 minutes. The formed sample is depicted in figure 8 (c).



(a)



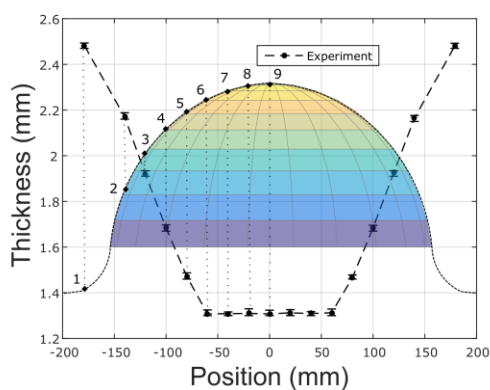
(b)



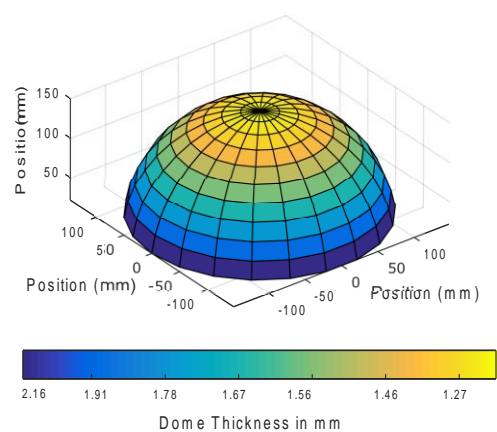
(c)

**Figure 8-** (a) experimental and polynomial approximation of the uniaxial stress-strain curve, from Jarrar et al. (2012), (b) numerical pressure curve and the approximated curve for the equipment and (c) the dome resulted by the SPF process.

Ultrasound inspection was used to evaluate the final thickness after superplastic forming. This result was important to give the maximum real thickness reduction and a reference in how strain field was distributed in sample's surface. Besides, both can be compared with analytical outputs. These results are shown in Figure 9.



(a)



(b)

**Figure 9-** Thickness distribution around the dome measured by the ultrasound technique.

This analysis shows a maximum thickness reduction of 51%. If compared with analytical prediction this value is about 35%, this difference is generated due to a limitation in the analytical model in representing the true stress-strain state which the material is subjected during the process. Additionally, it does not consider other intrinsic process phenomenon as

friction and thermal effects. In this case the use of more complex numerical methods such as finite elements would allow a better representation of the experimental case. It was possible to observe that the maximum reduction of thickness is homogenous in a considerable area near at the center of dome. This information is relevant in this context because it represents a substantial capacity of the process in distributing forging efforts without inducing local necking. In a preliminary analysis, it can indicate a macro behavior of grain boundary sliding, which is a characteristic of superplasticity, however some complementary tests are necessary to prove this argument.

It was also noted that the part do not reached the final expected height and, in order to explain this fact, the sample was analyzed by electronic microscopy inspection, as shown in Figure 10 and Figure 11.

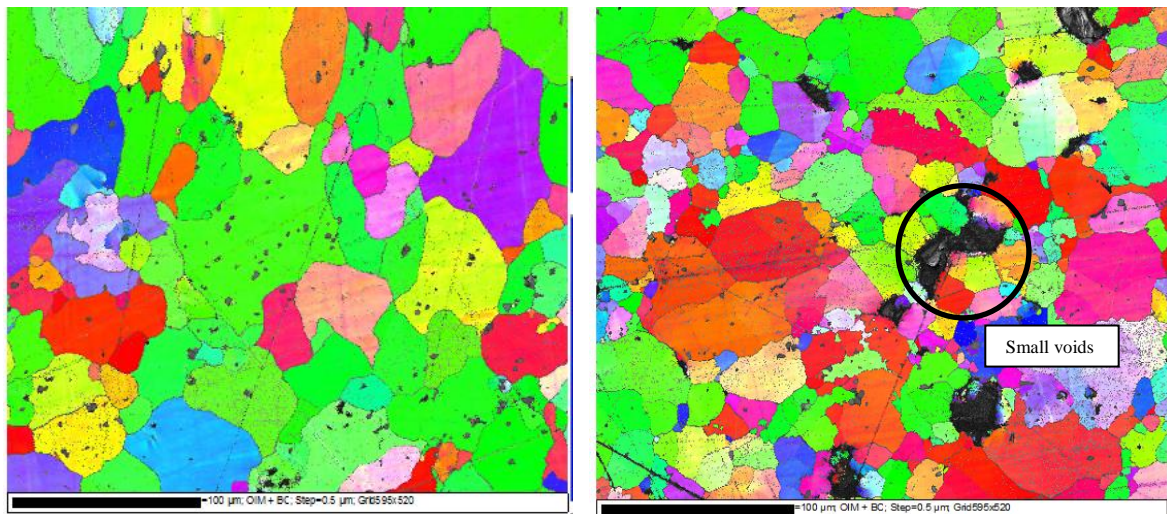


**Figure 10 – EBSD before and after forming.**

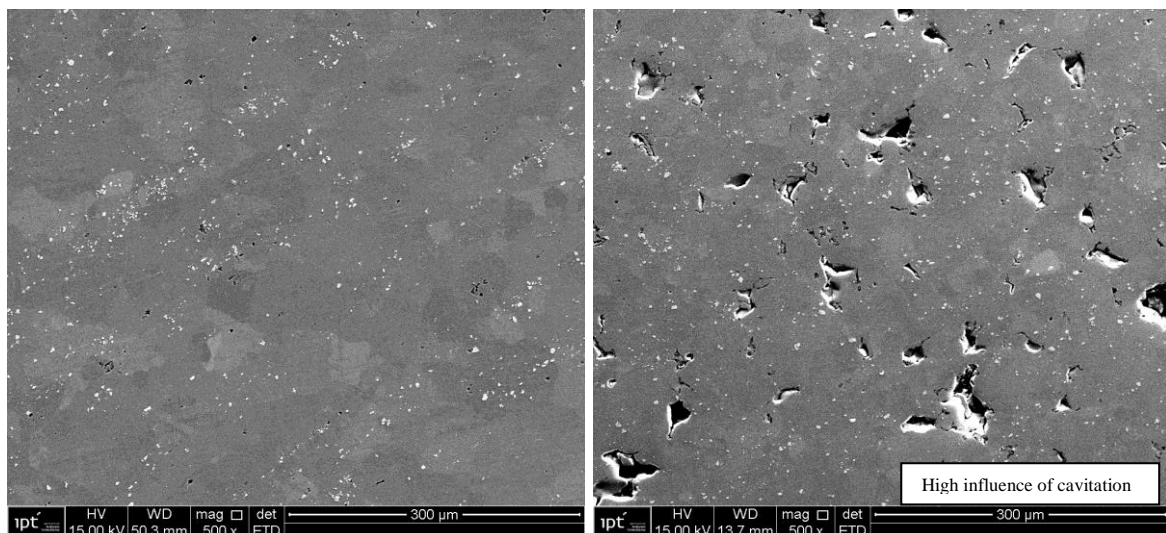


**Figure 11 – SEM before and after forming.**

The images show a formation of small voids in material structure which can be associated with loss of efficiency in superplastic expansion. This phenomenon can be called cavitation, which is a problem in most superplastic aluminum alloys.

## CONCLUSIONS

The results show that the predicted pressure curve obtained following the analytical approach is adequate to reach a low-velocity strain rate during the experiments. In that condition, the dome reaches the highest deformation after 51 min, which is an expected time for the SPF process according to the literature. However, the percentage of thickness reduction in the experimental and analytical model deviates, they are 51% and 35%, respectively, this variation occurs due to the limitation of the Mukherjee's analytical formulation, as an example it does not consider some of the intrinsic process phenomena such as friction and thermal effects.

It is noted by the electronic microscopy inspection that the size of the grain in the AA5083 sheet is higher than the grain size expected grain size for the SPF envelope. This result shows that the superplasticity can be obtained even when there are some parameters of the outside of the window. The dome didn't reach the final size due to the high influence of the cavitation phenomena, which is a serious problem that can be observed in the AA 5083 alloys. Even though, the thickness distribution is uniform around the dome, showing the high quality of this process.

Finally, from the literature, it is known that the use of superplastically formed 5083 aluminum alloys was confirmed as an acceptable and cost effective solution for many aerospace applications. Therefore, one can conclude that more studies in this area are necessary such as: (i) perform uniaxial analysis to obtain the best real SPF process envelope. (ii) apply the back pressure to avoid the cavitation phenomena and (iii) use the equal channel angular pressing process (ECAP) for decreasing the alloy grain size.

## REFERENCES

- Journal:** Aksenov, S. A., Chumachenko, E. N., Kolesnikov, A. V., & Osipov, S. A. 2015. "Determination of Optimal Gas Forming Conditions from Free Bulging Tests at Constant Pressure." *Journal of Materials Processing Technology*, 217, 158-164.
- Journal:** Alabort, E., Kontis, P., Barba, D., Dragnevski, K., & Reed, R. C. 2016. "On the Mechanism of Superplasticity in Ti – 6Al – 4V." *Acta Materialia*, 105, 449-463.
- Journal:** Barnes, A.J. 2007. "Superplastic Forming 40 Years and Still Growing." *Journal of Materials Engineering and Performance*, 16 (4): 440–54.
- Journal:** Barnes, A. J., Raman, H., Lowerson, A., & Edwards, D. 2012. "Recent Application of Superformed 5083 Aluminum Alloy in the Aerospace Industry." *Materials Science Forum*, 735, 361-371.
- Master's Thesis:** Deshmukh, P. V. 2003. "Study of Superplastic Forming Process Using Finite Element Analysis". University of Kentucky, Lexington, USA.
- Journal:** Dutta, A., & Mukherjee, A. K. 1992. "Superplastic Forming: An Analytical Approach." *Materials Science and Engineering A*, 157 (1): 9–13.
- Journal:** Gershon, B., Eldror, I., Arbel, I., & Milo, J. 2004. "Problems Encountered in

Superplastic Forming of Al 5083 Parts.” *Materials Science Forum*, 447-448: 259–264.

**Book:** Giuliano, G. 2011. *Superplastic Forming of Advanced Metallic Materials: Methods and Applications*. Elsevier.

**Journal:** Hefti, Larry D. 2007. “Commercial Airplane Applications of Superplastically Formed AA5083 Aluminum Sheet.” *Journal of Materials Engineering and Performance* 16 (2): 136–41.

**Journal:** Jarrar, F. S., L. G. Hector, M. K. Khraisheh, and K. Deshpande. 2012. “Gas Pressure Profile Prediction from Variable Strain Rate Deformation Paths in AA5083 Bulge Forming.” *Journal of Materials Engineering and Performance* 21 (11): 2263–73.

**Book:** Jones, R. M. 2009. *Deformation Theory of Plasticity*. Bull Ridge Corporation.

**Journal:** Kaibyshev, O. A. 2002. “Fundamental Aspects of Superplastic Deformation.” *Materials Science and Engineering: A* 324 (1-2): 96–102.

**Journal:** Kappes, J., & Liewald, M. 2011. “Evaluation of Pneumatic Bulge Test Experiments and Corresponding Numerical Forming Simulations.” *Journal of Materials Science and Engineering, B* 1: 472–78.

**Journal:** Kawasaki, M., & Langdon, T. G. 2007. “Principles of Superplasticity in Ultrafine-Grained Materials.” *Journal of Materials Science* 42 (5): 1782–96.

**Journal:** Meier, M. L., Lesuer, D. R., & Mukherjee, A. K. 1992. “The Effects of the  $\alpha/\beta$  Phase Proportion on the Superplasticity of Ti-6Al-4V and Iron-Modified Ti-6Al-4V.” *Materials Science and Engineering A*, 154 (2): 165–73.

**Journal:** Salishchev, G. A., Kudryavtsev, E. A., Zharebtsov, S. V., & Semiatin, S. L. 2012. “Low Temperature Superplasticity of Ti-6Al-4V Processed by Warm Multidirectional Forging.” *Materials Science Forum*, 735: 253–58. Meier

**Journal:** Sieniawski, J., & Motyka, M. 2007. “Superplasticity in Titanium Alloys.” *Journal of Achievements in Materials and Manufacturing Engineering*, 24 (1): 123–30.

**Journal:** Sun, P. H., Wu, H. Y., Lee, W. S., Shis, S. H., Perng, J. Y., & Lee, S. 2009. “Cavitation Behavior in Superplastic 5083 Al Alloy during Multiaxial Gas Blow Forming with Lubrication.” *International Journal of Machine Tools and Manufacture*, 49 (1): 13–19.